Non-exponential and oscillatory decays in quantum mechanics

Murray Peshkin[1], Alexander Volya[2] and Vladimir Zelevinsky[3]

[1] *Argonne National Laboratory, Physics Division, Argonne, Illinois 60439.*
[2] *Florida State University, Physics Department, Tallahassee, Florida 32306.*
[3] *National Superconducting Cyclotron Laboratory and Department of Physics and Astronomy, Michigan State University, East Lansing, Michigan 48824.*

arXiv:1703.05238v1 [nucl-th] 15 Mar 2017

PACS 03.65.Xp – Tunneling, traversal time, quantum Zeno dynamics

Abstract – The quantum-mechanical theory of the decay of unstable states is revisited. We show that the decay is non-exponential both in the short-time and long-time limits using a more physical definition of the decay rate than the one usually used. We report results of numerical studies based on Winter's model that may elucidate qualitative features of exponential and non-exponential decay more generally. The main exponential stage is related to the formation of a radiating state that maintains the shape of its wave function with exponentially diminishing normalization. We discuss situations where the radioactive decay displays several exponents. The transient stages between different regimes are typically accompanied by interference of various contributions and resulting oscillations in the decay curve. The decay curve can be fully oscillatory in a two-flavor generalization of Winter's model with some values of the parameters. We consider the implications of that result for models of the oscillations reported by GSI.

Introduction. – This paper presents our perspective on the quantum-mechanical theory of decaying states. In part of it we make use of Winter's solvable model, for which we have made numerical calculations. For brevity and to keep the perspective in focus, we frequently characterize the results of those calculations, presenting few details. Needed details will be published elsewhere.

The exponential decay of unstable states is one of the most pervasive and most studied phenomena in microscopic physics, yet its quantum-mechanical theory remains obscure in many ways.

The classical decay rate $R_c(t)$ is proportional to the available population of the unstable state and therefore to the classical survival probability $S_c(t)$,

$$R_c(t) \equiv -\frac{dS_c}{dt} = \Gamma\, S_c(t) \rightsquigarrow R_c(t) = \Gamma\, e^{-\Gamma t}. \qquad (1)$$

The constancy of Γ in Eq. (1) is responsible for exponential decay law. This description is based on the assumption that only the population, not the structure, of the parent state changes over time while the mechanism of decay of every member of the population is constant. More generally, the parent state could have substates, each with its own initial population and its own Γ. Then $R_c(t)$ would be a sum of decreasing exponentials with positive coefficients and it would decrease monotonically as function of time. Experiments have observed exponential decay over many half-lives. A detailed statistical analysis [1] shows that the exponential stage of beta-decay is indeed a random process.

No quantum-mechanical counterpart of Eqs. (1) with constant Γ is valid at all times. Many authors [2–15] have emphasized the generally non-exponential nature of decay laws in quantum mechanics, along with the problems of experimental observation of deviations from a pure exponential decay. The discussion has recently been revitalized by the reported observation of decay oscillations during times comparable with the half-life in neutrino emission [16, 17]. That observation remains to be fully confirmed but it has stimulated active theoretical discussions, for example [18–22], with the contributors taking diametrically opposite views. Evidence for non-exponential decay in the case of ^{14}C used for radioactive dating has been claimed and debated [23–25].

Textbook treatments of the subject vary but they appear all to be described accurately by the words of E. Merzbacher [2]: "*the exponential decay law ... is not a rigorous consequence of quantum mechanics but the result of somewhat delicate approximations.*" There is evidently something right about those delicate approximations because they do yield the correct exponential decay rates in some atomic physics cases where everything needed for

the calculation is known. However they are silent about the range of times during which the decay is exponential. Moreover, they define the survival probability of the initial state $\Psi(0)$as

$$S(t) = |\langle\Psi(0)|\Psi(t)\rangle|^2 . \tag{2}$$

That definition seems to us unrepresentative of what experiments really measure. $S(t)$ should be the probability of finding a parent nucleus or an excited atom at time t, not necessarily the probability of finding the system in exactly the state represented by $\Psi(0)$.

The presence of three regimes – initial, exponential, and long-time inverse power law – appears to be a universal feature of the decay process. The transitions from one regime to another are accompanied by the interference of corresponding quantum amplitudes seen as oscillations on the decay curve. Below we review different decay regimes. We also consider the possibility of more unusual oscillatory modes caused by quantum dynamics of populations of different substates.

Winter's model. – The physics of decay was clarified by Winter [26] with a potential model that has features resembling those of a real physical system. This model became a useful tool to study non-exponential features in decay [27, 28]. In Winter's model a particle of mass m moves in one dimension between an impenetrable wall at $x = -1$ and $x \to \infty$ under the influence of a confining potential $V(x) = G\delta(x)$. Taking $\hbar = 2m = 1$ Winter's Hamiltonian and its energy eigenfunctions $|k\rangle$ are given by

$$H_W = -\frac{\partial^2}{\partial x^2} + G\delta(x), \tag{3}$$

$$\langle x|k\rangle = \sqrt{\frac{2}{\pi}} \begin{cases} \frac{\sin(\phi_k)}{\sin(k)} \sin\left[k(x+1)\right], & -1 \le x < 0 \\ \sin(kx+\phi_k), & x \ge 0 \end{cases} . \tag{4}$$

where E is the energy, $k = \sqrt{E}$ is the asymptotic momentum, states $|k\rangle$ are normalized as $\langle k|k'\rangle = \delta(k-k')$, and $\cot(\phi_k) = \cot(k) + G/k$.

At time $t = 0$, the wave function $\Psi(x,t)$ is confined to the interior, or parent, region $x \le 0$. The survival probability is defined as

$$S_W(t) = \int_{-1}^{0} |\Psi(x,t)|^2 \, dx. \tag{5}$$

Winter solved the time-dependent Schrödinger equation for physically motivated values of the parameters by expanding the wave function in the complete set $|k\rangle$ to find that the decay rate $R(t)$ rises from zero at $t = 0$ in a time significantly shorter than the halflife, then settles into an exponential regime for many halflives, and finally goes over into the expected inverse power of t. (See also more accurate calculations by Dicus et. al. [27] and in the textbook [28] based on the same model.)

Winter's model presents an opportunity to test a consequence of Merzbacher's "delicate assumptions" Ref. [2]

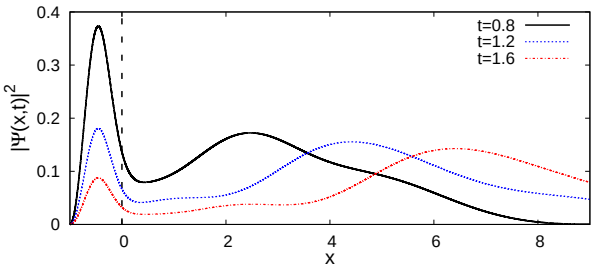

Fig. 1: Probability distribution $|\Psi(x,t)|^2$ for a decaying state at $t = 0.8$, 1.2, and 1.6. Here $G = 6$.

that lead to the expansion of the wave function in poles at complex energies. In our calculations we generally used that expansion, as did Winter. However we also applied direct numerical integration and obtained identical results.

The radiating state. – In our numerical calculations based on Winter's model, we have found that the parent wave function, i.e. the part of $\Psi(x,t)$ in the region $x < 0$, rapidly approaches what we call the "radiating state",

$$\Psi(x,t) \simeq \Psi_R(x)\, e^{-\Gamma t/2} e^{-iE_R t}, \tag{6}$$

and remains there throughout the exponential stage. The radiating state wave function $\Psi_R(x)$ is independent of the initial state and it remains constant in shape during the exponential regime. E_R in Eq.(6) is the average kinetic energy in $x < 0$ during the period of decay with rate Γ.

The radiating state provides the quantum-mechanical counterpart of the classical survival probability S_c of Eqs. (1) and it gives some justification for a key assumption in quantum-mechanical treatments that the rate of change of the amplitude for being in the parent state is proportional to that amplitude. Fig. 1 illustrates a typical example of a calculation. The wave function for $x < 0$ retains its shape as function of x.

The earliest times. – That the decay rate at time $t = 0$ must vanish has been proved under various assumptions [15], defining the survival probability as in Eq. (2), which as argued earlier is generally unphysical.

The proper definition depends on the experiment used to detect the parent or daughter state but in practice that appears never to be an issue. However that may be, let P be the projector on states in which a parent atom or nucleus is present and no daughter is present. The appropriate survival probability S and decay rate R are given by

$$S(t) = \langle P\Psi(t)|P\Psi(t)\rangle, \tag{7}$$

$$R(t) = -dS(t)/dt = -2\,\mathrm{Im}\left\{\langle P\Psi(t)H|(1-P)\Psi(t)\rangle\right\}. \tag{8}$$

If it is assumed that $(1-P)\Psi(0)$ vanishes, then

$$R(0) = 0. \tag{9}$$

This result is an exact consequence of the Schrödinger equation under the assumption, valid in the Winter model,

that there is a time $t = 0$ when the parent state is surely present and the daughter absent. In real physics that assumption, which is explicit or implicit in all derivations of Eq. (9) of which we know, can never be exact and its applicability varies with the application. An unstable nucleus may be created either by a reaction in some other channel whose participants are long gone at times of interest and need not be included in the calculation, or filtered by some experiment. In either case the process takes a finite time but that time is typically very short compared to times of physical interest and Eq. (9) is an excellent approximation. Then $R(t)$ rises from 0 at $t = 0$ before settling into an exponential or a sum of a few exponentials. For a long-lived resonance in a scattering process, Eq. (9) lacks even approximate validity. This derivation of Eq. (9) agrees with earlier work that used Eq. (2) if P is defined as the projection on $\Psi(0)$.

Effective non-Hermitian Hamiltonian. – Starting from diverse approaches [15, 29], the time behavior has been expressed as a squared Fourier integral $S(t) = |\mathcal{F}(t)|^2$, of some energy-dependent amplitude,

$$\mathcal{F}(t) = \int dE\, \exp(-iEt) D(E). \tag{10}$$

The function $D(E)$, closely related to the S-matrix, has resonance poles, $\mathcal{E}_r = E_r - \frac{i}{2}\Gamma_r$, in the lower part of the complex energy plane, $\Gamma_r > 0$.

The exponential time evolution of an initial quasi-stationary state corresponds to a single complex pole and to the Lorentzian energy spectrum of the decaying state,

$$|\Psi_E|^2 \propto \frac{\Gamma/2}{(E - E_r)^2 + \Gamma_r^2/4}, \tag{11}$$

Many features of time-dependent decay, including the short-time evolution, interference between resonances and decay at remote times, can be explored using the description in terms of the effective non-Hermitian Hamiltonian. This approach based on the Feshbach projection [30] has found wide applicability in various branches of science; examples and references can be found in a review article [31]. Explicit dynamics of many-body states in realistic nuclear systems was studied by this method in Ref. [32].

In this approach the Hilbert space is separated into intrinsic (or parent) part P and an external part, the states with the asymptotics of continuum channels. Then the function $D(E)$ in Eq. (10) emerges from the effective propagator that describes the evolution in the subspace P,

$$\mathcal{G}(E) = \frac{1}{E - \mathcal{H}}, \quad \mathcal{H} = H - \frac{i}{2} W. \tag{12}$$

The effective Hamiltonian $\mathcal{H}$ in Eq. (12) is energy dependent and, for energy E above thresholds, non-Hermitian, where the anti-Hermitian part W describes the loss of flux from the intrinsic space. The unitarity of the scattering matrix requires W to be factorized,

$$\langle 1|W|2\rangle = \sum_{c\,(\mathrm{open})} A_1^c A_2^c. \tag{13}$$

The amplitudes $A_1^c \equiv \langle c, E|H|1\rangle$ are the matrix elements of the original Hamiltonian between an intrinsic state $|1\rangle$ and the channel state $|c, E\rangle$. The channel state is labeled here by the asymptotic energy E and all additional quantum numbers are combined in label c. For convenience, in this formalism the channel states are normalized by delta function of energy $\langle c, E|c', E'\rangle = 2\pi\, \delta_{cc'}\, \delta(E - E')$. Therefore, the kinematic factors (density of states in the continuum for a given channel) are included in these amplitudes so that they depend on running energy E and vanish at the threshold of a given channel; only channels which are open at a given energy contribute to this on-shell part of the Hamiltonian. The resonances emerging from the poles of $\mathcal{G}(z)$ in the complex energy plane determine the analytic structure of the function D in Eq. (10).

Let us illustrate this approach with an example of one intrinsic state coupled to the continuum, Fig. 2. The survival amplitude for this state is given by the expectation value of the propagator (12) in the initial state $\Psi(0)$ that is assumed to be in the intrinsic space,

$$\mathcal{G}(E) = \frac{1}{E - E_0 + \frac{i}{2}\Gamma(E)}, \quad \text{where} \quad \Gamma(E) = A^2(E). \tag{14}$$

The energy dependence of amplitudes at low energies follows from decay width being proportional to the density of states; for spherically symmetric s-wave decay $\Gamma(E) \propto \int d^3k\, \delta(E - k^2) \propto \sqrt{E}$. If the state is far from the threshold and the energy dependence of Γ is ignored, this propagator $\mathcal{G}(E) = 2\pi D(E)$ represents the exponential time evolution of the initial state with a Breit-Wigner cross section, Fig. 2.

Pre-exponential dynamics. – At short times the wave function can contain multiple components reflecting the structure distributed among many resonant poles. The pre-exponential dynamics involves transitions between these states and radiation with different exponential rates finally leaving a single exponential term corresponding to the pole closest to the real axis. Internal transitions influence the survival probability of Eq. (2) whereas the total radiation is measured by Eq. (7).

Consider two overlapping resonances described by the general non-Hermitian Hamiltonian, [33],

$$\mathcal{H} = \begin{pmatrix} \epsilon_1 - (i/2)\Gamma_1 & v - (i/2)A_1A_2 \\ v - (i/2)A_1A_2 & \epsilon_2 - (i/2)\Gamma_2 \end{pmatrix}. \tag{15}$$

Here $\epsilon_{1,2}$ are diagonal elements of the Hermitian part H and v is the internal mixing; the non-Hermitian part W contains $\Gamma_{1,2} = A_{1,2}^2$ where the amplitudes $A_{1,2}$ are real and in general dependent on running energy E. The cross section of the resonance reaction and the survival probability for this model are shown in Fig. 3.

In the limit of separated resonances far from the threshold, the behavior and decay curves are nearly identical to those for a single state, Fig. 2. When the states are close to each other, their mixing and interference occur via both

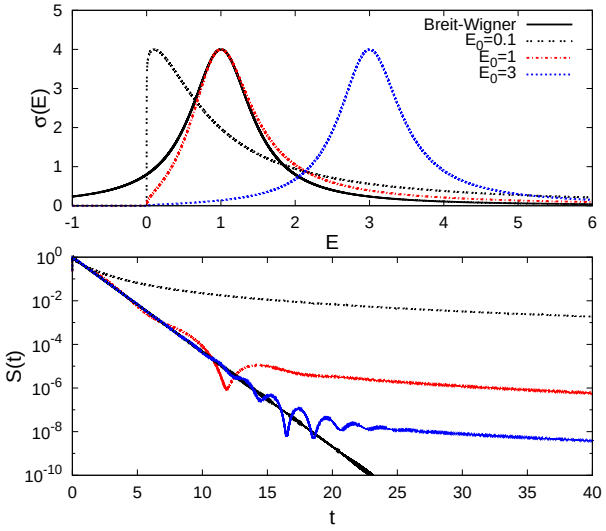

Fig. 2: Single resonance near threshold. Top panel energy-dependent scattering cross section off a resonance. Lower panel the survival probability as a function of time. The Breit-Wigner resonance with the Lorentzian shape, Eq. (11), would correspond to pure exponential decay. The realistic resonances at different positions E_0 are modeled with energy-dependent Breit-Wigner s-wave kinematics and cross section going to zero at threshold.

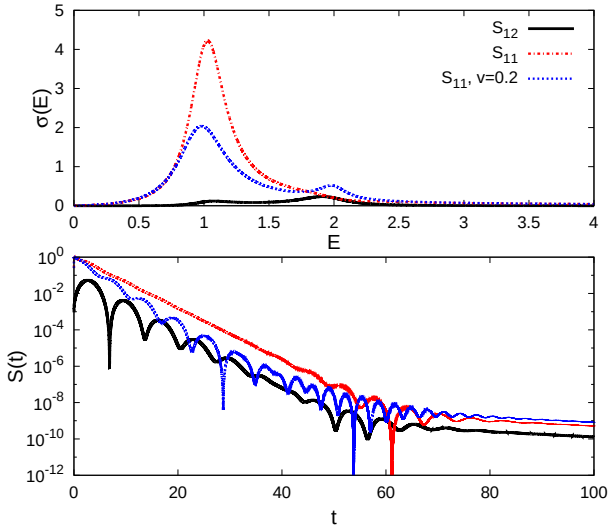

Fig. 3: Two-state model for the effective Hamiltonian (15). Top panel: shows the energy-dependent cross section. Lower panel: the survival probability as a function of time. Here $\epsilon_1 = 1$, $\epsilon_2 = 2$; $\Gamma_1(E) = \Gamma_2(E) = \sqrt{0.1E}$. The curve S_{11} shows the survival probability for the first intrinsic state, and S_{12} the probability for transition $2 \to 1$; $v = 0$ in these cases. The third curve illustrates the behavior S_{11} in the mixed case $v = 0.2$ for amplitudes having opposite signs.

Hermitian and non-Hermitian part resulting in the oscillatory modulation of the survival probability with beat times $t \sim 1/|\epsilon_1 - \epsilon_2|$. Such oscillations reflect internal transitions in the decaying system with two radiating states mixed by internal interactions, Fig. 3. Oscillations in the decay rate can emerge only if the two radiating states have different decay rates. At remote times determined by the decay width and the distance to the threshold, the model recovers the asymptotic power-law behavior discussed below.

In Winter's model the internal dynamics is determined by matrix elements of the evolution operator,

$$M_{nn'}(t) = \langle n|e^{-iHt}|n'\rangle = \int_0^\infty e^{-ik^2 t}\langle n|k\rangle\langle k|n'\rangle dk, \quad (16)$$

where a complete set of intrinsic states for $x \in [-1, 0]$ is defined as $\langle x|n\rangle = \sqrt{2}\sin[n\pi(x+1)]$ with $n = 1, 2, \ldots$. The survival probabilities for individual states are $S_{nn}(t) = |M_{nn}(t)|^2$. The analytic properties of the functions $D_{nn} = \langle n|k\rangle\langle k|n\rangle$ are seen from Eq. (4). The poles $E_r = k_r^2$ correspond to the roots of the equation $k^2 + k\,G\sin(2k) + G^2\sin^2(k) = 0$. In Eq. (10) the integration contour in the complex energy plane for $t > 0$ should be drawn in the fourth quadrant and closed on the real axis at the threshold point $E = E_{\rm th}$. Integration in Eq. (16) (where $E_{\rm th} = 0$) gives rise to two types of contributions, the terms responsible for exponential decay from the poles k_r and the non-exponential component $M_{nn'}^{(NR)}(t)$ from the Gaussian-type integral along the vertical boundary of the fourth quadrant ($\mathrm{Re}\, E = 0$),

$$M_{nn'}(t) = \sum_{k_r} M_{nn'}^{(r)}\, e^{-ik_r^2 t} + M_{nn'}^{(NR)}(t). \quad (17)$$

Here the resonance amplitudes, $M_{nn'}^{(r)}(t) = -2\pi i\,\mathrm{Res}(k_r)$, given by the residues at the poles, determine exponential dynamics, $\Gamma_r \equiv 1/\tau_r = -2\mathrm{Im}(k_r^2)$. The non-resonant contribution follows from the direct integration; in the large time limit

$$M_{nn'}^{(NR)}(t) = \frac{1+i}{\pi^{5/2}\sqrt{2}}\,(1+G)^2\,\frac{1}{nn'}\,\frac{1}{t^{3/2}}. \quad (18)$$

During the initial evolution the survival probability is a collection of radiating exponents, the sum over poles k_r in Eq. (17). This is highlighted in Fig. 4 where the survival probability is shown for the initial state $n = 2$. This state has only a small $r = 1$ component $M_{22}^{(1)} = 0.0005$ and a very large $r = 2$ component $M_{22}^{(2)} = 0.9917$. Thus, at short times the decay follows $\exp(-t/\tau_2)$ until the resonant component corresponding to τ_2 dies out. The amplitudes associated with $r = 1$ and $r = 2$ poles become similar at $t \approx 1$ in Fig. 4; then the two decay modes interfere. The transition to the pure $\exp(-t/\tau_1)$ decay law ends the pre-exponential dynamics.

The details of the pre-exponential regime depend on the disposition of poles, on the exact form of the initial wave function, as well as on the quantity observed as a decay signal. The resulting behavior is shown in Fig. 5.

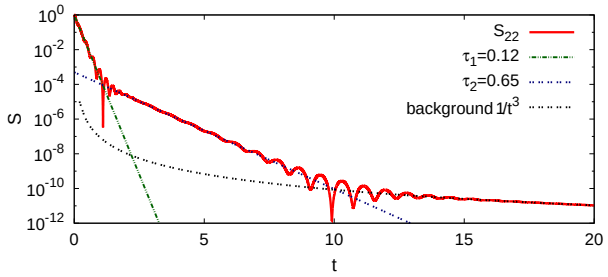

Fig. 4: Survival probability $P_{22}(t)$ as a function of time. For $G = 6$, the two lowest complex poles are at $k_1 = 2.75794 - i\,0.140433$ ($\tau_1 = 0.65$) and $k_2 = 5.71348 - i\,0.370148$ ($\tau_2 = 0.12$), their resonant contributions are shown along with the non-resonant background from Eq. (18).

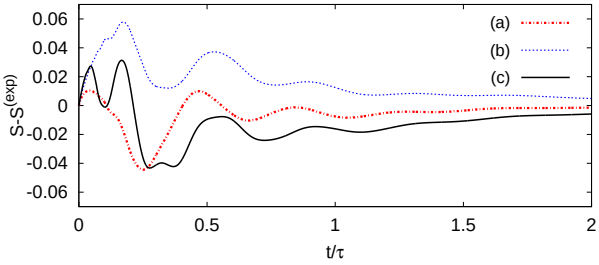

Fig. 5: Difference between the actual survival probability and $S(\exp) = \exp(-t/\tau)$, where $\tau = \tau_1$ is the leading term in Eq. (16), $G = 6$. The time is expressed in units of the lifetime τ. Curve (a): deviation of $S_{11}(t)$ from the exponent. Curve (b) corresponds to $S(t)$ from Eq. (7) where intrinsic space P is defined as $x \in [-1, 0]$. Curve (c) is the same as (b) but for the initial wave function with finite ΔE, $\Psi(x, 0) = \sqrt{8/3}\,\sin^2(\pi x)$.

Decay rate at long times. – Deviations from exponential decay are also expected in the post-exponential long-time limit, when resonant sources dry out leaving only the non-resonant component with its characteristic power-law time dependence as seen in Fig. 4. The transitional region around $t = 10$ is associated with the interference of exponential and power-law terms.

The non-exponential long-time behavior comes from the fact that the energy spectrum has a lower bound. The exponential decay implies Lorentzian in energy spectrum with an unphysical tail to infinitely low energies. As the physical spectrum of a given decay channel starts at a threshold, let say $E_{\rm th} = 0$, the exponential stage with $\tau \sim 1/\Gamma$ is expected to end at $t \sim t_L$ when

$$e^{-t_L/\tau} \sim \frac{E_0}{\Gamma} \quad \rightsquigarrow \quad t_L \sim \tau \,\ln\left(\frac{E_0}{\Gamma}\right). \tag{19}$$

At $t \to \infty$, the behavior of $D(E)$ at threshold, $E \to E_{\rm th}$, related to the physics of non-resonant particles near the lowest energy, defines the time dependence of decay. Close to threshold, $D(E)$ is determined by the density of states in the continuum, typically $D(E) \propto (E - E_{\rm th})^\lambda$. For a neutral particle with orbital momentum ℓ leaving a spherically symmetric potential, $\lambda = \ell + (1/2)$. This contribution to $\mathcal{F}(t)$ is proportional to $1/t^{\lambda+1}$, so that the asymptotic power law for $|\mathcal{F}(t)|^2$ is $\propto 1/t^{2\lambda+2}$, or $1/t^3$ for the s-wave.

Fig. 2 illustrates how the threshold at $E_{\rm th} = 0$ distorts the Lorentzian and eliminates exponential decay. Here the s-wave behavior of the decay width, $\Gamma(E) \propto \sqrt{E}$, is assumed. The transition time t_L depends on the distance to the threshold as illustrated by Fig. 2. The decay width $\Gamma(E)$ is proportional to the phase space volume and thus also scales as a power law. The power-law feature is correctly recovered in the effective Hamiltonian approach leading to $S(t) \sim 1/t^{2\ell+3}$.

Alternatively, we can say that the initial internal state, being coupled to the continuum, is not stationary and thus contains the low-energy components of the continuum; the power-law decay emerges due to the slowest particles present in this wave function [6, 34]. The outgoing background can be noticed in Fig. 1. In this logic, see also [6], one can say that at time t the number of free particles of mass m and velocity v in the region $\Delta x \sim 1/(mv)$ is

$$S(t) \propto \frac{\Delta x}{vt} \sim \frac{1}{mv^2 t} = \frac{2}{E_0 t} \propto |\Psi(t)|^2\,. \tag{20}$$

This semiclassical argument implies a $1/t$ power-law for the survival probability. In quantum mechanics the features of low-energy scattering with $1/t^3$ for s-wave should be used in place of such semiclassical arguments. Even for a very small non-resonant component in the initial state, it decays slower than the resonant part. At time $t \sim t_L$ the resonant and non-resonant components become comparable and for $t > t_L$ decay becomes non-exponential. Because of a tiny amount of decaying material left after many lifetimes, this stage is hard to observe experimentally. But in the transitional region the resonance and threshold contributions are of the same order and interfere so that the transition to the power law is accompanied by characteristic oscillations seen in numerical simulations.

Flavor oscillation model. – On the wave of the GSI experiments [16, 17] it has been speculated that mixing of two close-in-energy radiating states could lead to exponential decay modulated by oscillations. The main difference with our previous discussion is the presence of two intermixed decay channels. We consider a flavor-mixing model

$$\begin{pmatrix} \nu_+ \\ \nu_- \end{pmatrix} = \begin{pmatrix} \cos\theta & \sin\theta \\ -\sin\theta & \cos\theta \end{pmatrix} \begin{pmatrix} \nu_1 \\ \nu_2 \end{pmatrix}, \tag{21}$$

where + and - subscripts denote upper and lower flavor states and subscripts 1 and 2 denote mass eigenstates. The kinetic part $\hat{K}$ of the Hamiltonian is diagonal in the mass eigenstates and can be written as

$$\hat{K}\nu_{1,2}(x) = \left[-\frac{\hbar^2}{2m_{1,2}}\frac{d^2}{dx^2} \pm \Delta\right]\nu_{1,2}(x), \tag{22}$$

where Δ is the difference in the rest masses. We assume that the potential barrier is diagonal in the flavor basis,

$$\hat{V}\nu_\pm(x) = G_\pm\,\delta(x)\,\nu_\pm(x). \tag{23}$$

For equal masses and identical potentials for both flavors, the problem is diagonal in the mass eigenstates and oscillations occur only between the flavor basis states which is not related to the decay process. While the flavor oscillations would be evident with definition (2), there are no decay oscillations associated with the probability to find the particle, independently of flavor, in the intrinsic space. In order for non-trivial oscillations to occur with the realistic definition (7), there should be a substantial difference between the decay rates into the two flavor states. The largest non-exponential effect is expected at the maximum mixing angle $\theta = 45°$. With G_+ fixed, we explore the extreme situations with $G_- = 0$ and $G_- = \infty$.

In Fig. 6 the probability to find a particle of any flavor in the $x < 0$ region is shown as a function of time for various parameters. All curves exhibit exponential decay. The average lifetime is governed by the combination of the barrier strengths. For $G = 6$ in Winter's model the mean lifetime $\tau = 0.65$; for the two-flavor model with equal masses and one flavor state not held by the barrier, $G_- = 0$, the lifetime drops to $\tau \approx 0.25$ (dotted line); the post-exponential regime is quickly reached around $t = 4$. In the opposite limit with $G_- = \infty$, the forbidden decay in the lower flavor state extends the lifetime to $\tau \approx 2$ which is nearly the same for equal masses $m_1 = m_2 = 0.5$ and $\Delta = 10$ (dashed-dotted line) and for $m_1 = 0.1$, $m_2 = 1$, and $\Delta = 0$ (double-dotted line).

In the limit where the decay in one of the flavor states is not hindered by a potential, $G_- = 0$, the flavor oscillations lead to the continuous modulation of the total (sum of both flavors) survival probability (solid line and dotted line in Fig. 6). Unlike in previous situations, these oscillations extend over multiple lifetimes being determined by the mass difference Δ; the period π/Δ is seen on inset. The presence of two decay channels is the principal difference in this case.

Conclusions. – Although many elements of our discussion are well known, being spread over the literature, it is useful to revisit the typical features of quantum decay of unstable states. In recent literature the nature and universality of the exponential decay has been questioned. Is exponential decay a result of some "delicate" approximations that may break down in certain limits? Is it possible to have an oscillatory decay behavior? We have examined several models, targeting their general analytic properties as well as showing exact numerical solutions. Our main conclusions can be summarized as follows:

• The formation of the radiating state that corresponds to the pole of the decay amplitude closest to the real axis is preceded by a short-time stage with low decay probability. The short-time limit can be sensitive to the details of the preparation of the unstable state (the experimental attempts were inconclusive [35–37]). However, the radiating state concept appears to be universal.

• The general theoretical approach based on the effective non-Hermitian Hamiltonian highlights the coupling of internal and external features.

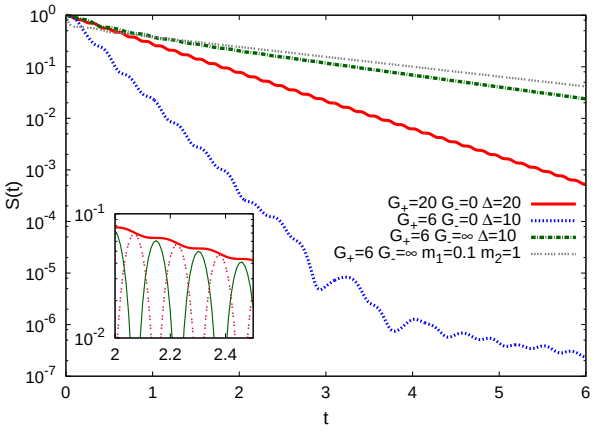

Fig. 6: Total survival probability as a function of time for the two-flavor model. The mixing angle is $\theta = 45°$. Other parameters of the Hamiltonian are indicated with labels. The initial state is assumed to be in the upper flavor with the $n = 1$ wave function of an infinite box. Inset shows oscillations of the survival probability for two flavor components and the combined total for $G_+ = 6$, $G_- = \infty$, $\Delta = 20$.

• The energy dependence of the decay amplitudes, in particular due to the proximity of channel thresholds, is responsible for the power-law decay tail that in the limit of long time wins over the main exponent while the transitional stage reveals oscillations.

• The two-flavor model shows that, for some sets of parameters, the entire decay curve is essentially oscillatory. Thus the possibility of observing oscillations in the decay process cannot be excluded. This result goes beyond the common scenario in which two states of the parent system are mixed by an external field so that their amplitudes in the wave function oscillate and the decay curve may oscillate with them. Here the two are mixed only indirectly by their coupling to the daughter states and the oscillations are not dependent upon external fields. However, a more realistic model will be needed to determine whether the analogous coupling in neutrino emission causes similar oscillations.

* * *

This work is supported by the U.S. Department of Energy, Office of Nuclear Physics, under contracts DE-AC02-06CH11357 and de-sc0009883, and by the NSF grants PHY-1068217 and PHY-1404442. We thank Yu. Litvinov for information concerning the GSI experiment.

REFERENCES

[1] M.P. Silverman, EPL **87**, 32001 (2009).
[2] E. Merzbacher, *Quantum Mechanics* (Wiley & Sons, New York, 1998).
[3] L.A. Khalfin, Dokl. Akad. Nauk USSR **115**, 277 (1957).

[4] L.A. Khalfin, Zh. Eksp. Teor. Fiz. **33**, 1371 (1957) [Sov. Phys. JETP **6**, 1053 (1958).]
[5] J. Schwinger, Ann. Phys. **9**, 169 (1960).
[6] R. Newton, Ann. Phys. **14**, 333 (1961).
[7] M.V. Terent'ev, Ann. Phys. **74**, 1 (1972).
[8] Ya.S. Greenberg, Izvestia Vuzov No. 12, 38 (1972).
[9] C.A. Nicolaides and D.R. Beck, Phys. Rev. Lett. **38**, 683 (1977).
[10] A. Peres, Ann. Phys. **129**, 33 (1980).
[11] G. Garcia-Calderón, J.L. Mateos, and M. Moshinsky, Ann. Phys. **249**, 430 (1996).
[12] R. Alzetta and E. D'Ambrogio, Nucl. Phys. **82**, 683 (1966).
[13] A.I. Baz', Ya.B. Zeldovich, and A.M Perelomov, *Scattering, reactions and decay in nonrelativistic quantum mechanics* (Nauka, Moscow,1966) [English translation: Israel Program for Scientific Translations, Jerusalem, 1969).
[14] H. Ekstein and A.J.F. Siegert, Ann. Phys. **68**, 509 (1971).
[15] L. Fonda, G.C. Ghirardi, and A. Rimini, Rep. Prog. Phys. **41**, 587 (1978).
[16] Yu.A. Litvinov *et al.*, Phys. Lett. B **664**, 162 (2008).
[17] P. Kienle *et al.*, Phys. Lett. B **726**, 638 (2013).
[18] A. N. Ivanov and P. Kienle, Phys. Rev. Lett. **103**, 062502 (2009)
[19] V.V. Flambaum, Phys. Rev. Lett. **104**, 159201 (2010).
[20] A. N. Ivanov and P. Kienle, Phys. Rev. Lett. **104**, 150202 (2010)
[21] A. Gal, Nucl. Phys. A 842, 102 (2010); arXiv:1407.1789.
[22] I.M. Pavlichenkov, Phys. Rev. C **81**, 051602(R) (2010).
[23] P.J. Aston, EPL **97**, 52001 (2012).
[24] A. Nicolaides, EPL **101**, 42001 (2013).
[25] P.J. Aston, EPL **101**, 42002 (2013).
[26] R.G. Winter, Phys. Rev. **123**, 1503 (1961).
[27] D.A. Dicus, W.W. Repko, R.F. Schwitters, and T.M. Tinsley, Phys. Rev. A **65**, 032116 (2002).
[28] V. Zelevinsky, *Quantum Physics*, vol. 2 (Wiley, Weinheim, 2011).
[29] J.G. Muga, G.W. Wei, and R.F. Snider, Ann. Phys. **252**, 336 (1996).
[30] H. Feshbach, Ann. Phys. **5**, 357 (1958); **19**, 287 (1962).
[31] N. Auerbach and V. Zelevinsky, Rep. Prog. Phys. **74**, 106301 (2011).
[32] A. Volya, Phys. Rev. C **79**, 044308 (2009).
[33] A. Volya and V. Zelevinsky, Phys. Rev. C **67**, 054322 (2003).
[34] E. Torrontegui, J.G. Muga, and J. Martorell, Adv. Quant. Chem. **60**, 486 (2010).
[35] E. Norman *et al.* Phys. Rev. Lett. **60**, 2246 (1988).
[36] E. Norman *et al.* Phys. Lett. B **357**, 521 (1995).
[37] W.W. Scates, D.P. Wells, J.F. Harmon, and R.J. Spraulding, in *CP680, Applications of Accelerators in Reseacrh and Industry*, ed. by J.L. Duggan and I.L. Morgan (AIP, 2003).